Design and characterization of a laterally mounted phased-array transducer breast-specific MRgHIFU device with integrated 11-channel receiver array

A. Payne,[a] R. Merrill, and E. Minalga
Utah Center for Advanced Imaging Research, University of Utah, 729 Arapeen Drive, Salt Lake City, Utah 84108

U. Vyas
Department of Bioengineering, University of Utah, 36 South Wasatch Drive, Salt Lake City, Utah 84112

J. de Bever
Department of Computer Science, 50 South Central Campus Drive, Salt Lake City, Utah 84112

N. Todd and R. Hadley
Utah Center for Advanced Imaging Research, University of Utah, 729 Arapeen Drive, Salt Lake City, Utah 84108

E. Dumont,
Image Guided Therapy, Inc., 2, Allee du Doyen Brus, Pessac 33600, France

L. Neumayer
Huntsman Cancer Institute, 2000 Circle of Hope Drive, Salt Lake City, Utah 84112

D. Christensen
Department of Bioengineering, University of Utah, 36 South Wasatch Drive, Salt Lake City, Utah 84112

R. Roemer
Department of Mechanical Engineering, University of Utah, 50 South Central Campus Drive, Salt Lake City, Utah 84112

D. Parker
Utah Center for Advanced Imaging Research, University of Utah, 729 Arapeen Drive, Salt Lake City, Utah 84108

(Received 13 August 2011; revised 26 January 2012; accepted for publication 28 January 2012; published 28 February 2012)

Purpose: This work presents the design and preliminary evaluation of a new laterally mounted phased-array MRI-guided high-intensity focused ultrasound (MRgHIFU) system with an integrated 11-channel phased-array radio frequency (RF) coil intended for breast cancer treatment. The design goals for the system included the ability to treat the majority of tumor locations, to increase the MR image's signal-to-noise ratio (SNR) throughout the treatment volume and to provide adequate comfort for the patient.

Methods: In order to treat the majority of the breast volume, the device was designed such that the treated breast is suspended in a 17-cm diameter treatment cylinder. A laterally shooting 1-MHz, 256-element phased-array ultrasound transducer with flexible positioning is mounted outside the treatment cylinder. This configuration achieves a reduced water volume to minimize RF coil loading effects, to position the coils closer to the breast for increased signal sensitivity, and to reduce the MR image noise associated with using water as the coupling fluid. This design uses an 11-channel phased-array RF coil that is placed on the outer surface of the cylinder surrounding the breast. Mechanical positioning of the transducer and electronic steering of the focal spot enable placement of the ultrasound focus at arbitrary locations throughout the suspended breast. The treatment platform allows the patient to lie prone in a face-down position. The system was tested for comfort with 18 normal volunteers and SNR capabilities in one normal volunteer and for heating accuracy and stability in homogeneous phantom and inhomogeneous *ex vivo* porcine tissue.

Results: There was a 61% increase in mean relative SNR achieved in a homogeneous phantom using the 11-channel RF coil when compared to using only a single-loop coil around the chest wall. The repeatability of the system's energy delivery in a single location was excellent, with less than 3% variability between repeated temperature measurements at the same location. The execution of a continuously sonicated, predefined 48-point, 8-min trajectory path resulted in an ablation volume of 8.17 cm^3, with one standard deviation of 0.35 cm^3 between inhomogeneous *ex vivo* tissue samples. Comfort testing resulted in negligible side effects for all volunteers.

Conclusions: The initial results suggest that this new device will potentially be suitable for MRgHIFU treatment in a wide range of breast sizes and tumor locations. © *2012 American Association of Physicists in Medicine*. [DOI: 10.1118/1.3685576]

Key words: high intensity focused ultrasound, MRI, breast

I. INTRODUCTION

The treatment of locoregional breast cancer has evolved from radical mastectomy to targeted local breast conserving therapy. The next logical step in this evolution is less invasive (nonsurgical) image-guided treatment of tumors. Various minimally invasive heating techniques (i.e., radio frequency ablation,[1,2] laser ablation,[3,4] cryoablation,[5,6] as well as noninvasive high-intensity focused ultrasound[7–16]) are currently under study in animal and human trials. While performing any of these procedures under MRI guidance can provide real-time images to improve procedure accuracy, magnetic resonance-guided high-intensity focused ultrasound (MRgHIFU) is a breast conserving therapy that can ablate tissue completely noninvasively. MRgHIFU offers many other advantages, including the avoidance of infections and scar formation, less required anesthesia, reduced recovery time, minimized normal tissue damage, and reduced systemic effects and costs.[9]

Several MRgHIFU breast treatment feasibility studies have been completed. In most of these cases,[8,12,13,17] the system used requires the patient to lie prone on the MRgHIFU device and the ultrasound beam is propagated vertically into the treatment region. These trials have provided evidence that MRgHIFU of the breast is feasible, but do not provide sufficient data to assess the effectiveness of MRgHIFU for treatment of the breast due to inherent limitations in the instrument design. Specifically, Furusawa *et al.*[12] reported that certain regions in the breast could not be ablated due to the "sonication prohibition" resulting from the ultrasound beam propagating through surgical scars or dimples in the skin, resulting in a vertical shift in the focal spot. An additional disadvantage of currently used vertically propagating systems that compress the treated breast against a membrane is the lack of optimum MR coils to image the breast since the systems can only accommodate a horizontal circular coil around the chest wall.

In order to overcome accessibility obstacles, a few HIFU systems have used laterally shooting transducers designed specifically to improve safety and enhance coverage in breast HIFU. For example, simulations of a breast-specific cylindrical ultrasound phased-array were performed on a breast model and initial phantom experiments were completed using a cylindrically mounted single solid transducer that was mechanically rotated.[18,19] The first laterally shooting HIFU transducer system to be used in malignant tissue on a patient[9] was not used beyond the initial feasibility study. A recent report[20] described a laterally shooting 384-element phased-array transducer for breast MRgHIFU treatments.

In this work, the design and preliminary evaluation of a laterally mounted phased-array breast-specific MRgHIFU device is presented that integrates several features intended to improve the treatment efficacy and safety of MRgHIFU in the breast. The design allows treatment of a large volume of the breast, increases signal-to-noise ratio (SNR) throughout the entire breast volume and provides adequate patient comfort for a MRgHIFU treatment.

II. METHODS

II.A. Breast system design description

The breast-specific MRgHIFU device presented in this work is composed of three main components: (1) a laterally propagating 256-element phased-array transducer mounted on the treatment cylinder using a custom rotational and pivotal support, (2) a custom 11-channel radio frequency (RF) coil array fitted around the treatment cylinder, and (3) a patient treatment platform that contains the device and supports the patient while being treated in the scanner. The transducer is driven by a power generator system designed and constructed by Image Guided Therapy (Bordeaux, France). The ultrasound power generator is designed to operate within the MRI scanner room and is shielded to eliminate interactions with the MRI signals. The ultrasound control computer is located outside the MRI scanner room and the control lines penetrate the room via optical fibers. The system was specifically designed for the Siemens 3 T Trio (60-cm bore) for placement directly onto the existing patient table (49-cm wide) but is also expected to be compatible with any MRI system with appropriate table size. Photographs of the system with the patient platform in place and removed are shown in Fig. 1. A 1-in. thick memory foam pad is placed over the patient platform and additional wedge-shaped cushions are used to position the patient in the device.

The patient lies prone on the device with the treated breast suspended in a 17-cm diameter treatment cylinder with the transducer mounted outside the main cylinder volume (Fig. 1). The contralateral untreated breast lies moderately compressed against contoured pads. The system is symmetric, allowing either breast to be treated individually. A window is cut out of the side of the treatment cylinder providing an acoustic window for the propagating ultrasound beam. The treatment cylinder is positioned underneath the patient platform on a pivotal support, allowing the cylinder to be

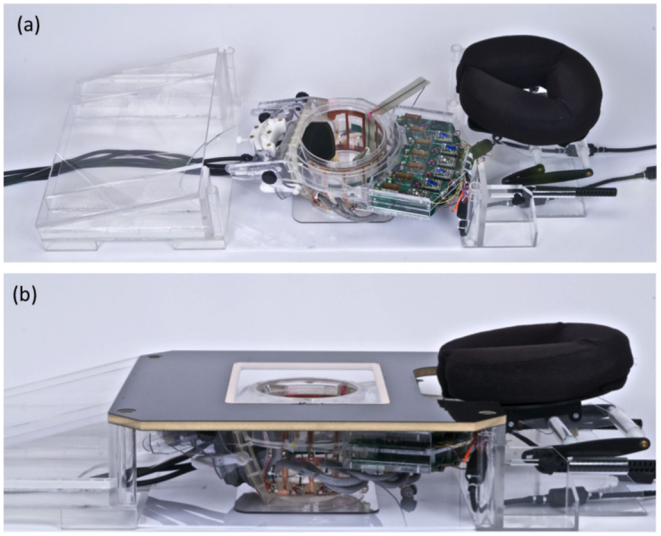

FIG. 1. Breast-specific MRgHIFU system shown (a) with the patient platform removed and (b) with the patient platform in place. The contoured body pads are not shown.

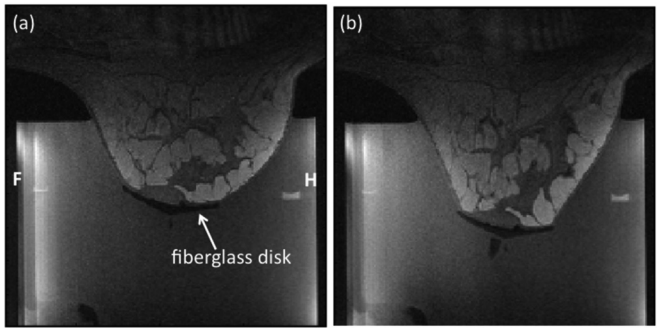

FIG. 2. Sagittal MRI images of a normal volunteer with the breast (a) suspended freely in the water-filled treatment cylinder and (b) with mild vertical tension applied. The patient is positioned head first, prone in the bore. Head (H) and foot (F) orientations are labeled in (a). Images were obtained using the 11-channel integrated RF coil array. The field of view is 183 × 183 mm.

positioned under the patient to accommodate variations in patient's anatomy.

A breast-tensioning device is incorporated into the tank to counteract the buoyancy effects that occur when the breast is suspended in the degassed water inside the cylinder. A fiberglass disk is placed over the nipple of the treated breast, secured with double-sided adhesive strips. A nylon cord is secured to the disk and mild tension is applied to the breast after the patient is positioned on the device. Figure 2 shows example MRI images of a breast from a normal volunteer in the treatment cylinder with and without tension applied.

II.B. Phased-array transducer and positioner

The system was designed to have electronic focal zone steering capabilities of approximately 1.5 cm in all directions[21] in order to treat a 3-cm diameter spherical lesion without having to mechanically move the transducer. Using lesion size as the metric, this would allow the treatment of approximately two-thirds of lesions in a study that was comprised of more than 24 000 breast cancer cases,[22] assuming that the geometric focus of the system is centered in the tumor. To meet this steering criterion, a phased-array transducer operating at 1 MHz was designed and constructed (Imasonic, Besançon, France). The transducer has 256, 4-mm diameter elements that are randomly positioned[23,24] over a section of a 10-cm radius sphere that is bounded by an aperture of 14.4 × 9.8 cm. The maximum power density available (based on the manufacturer's recommendation) is 2 W/cm^2.

The transducer is mounted laterally to the treatment cylinder, as shown in Fig. 3(a). This transducer-cylinder assembly has three degrees of freedom. The entire assembly can be rotated 145° around the treated right breast and 152° around the treated left breast (the asymmetry is due to limitations of cable flexibility). The transducer is able to rotate further around its geometric focus by ± 7.5°. The transducer can be tilted in the plane perpendicular to the MR table (in the anterior–posterior direction) by ±22° around a nominal axis oriented at 17° with respect to the horizontal. Finally, the transducer can be moved 5.7 cm total along the slot guide, toward and away from central axis of the cylinder. The focal spot can be placed at the midpoint of the treatment cylinder's axis by tilting the transducer down 15° from the 17° nominal axis and retracting the transducer 0.6-cm out of the treatment cylinder. The entire volume that can be treated within the cylinder when including the electronic steering capabilities of the transducer is shown in Figs. 3(b) and 3(c). A schematic of a normal volunteer's breast (12-cm length, 15.6-cm diameter) is shown in Fig. 3(b). All mechanical manipulation of the transducer position is performed manually. Several registration marks and metrics are located on the treatment cylinder and patient platform to ensure repeatable placement of the transducer. The transducer is coupled to the cylinder using a plastic bellows, as seen in Fig. 3. Deionized, degassed water is used

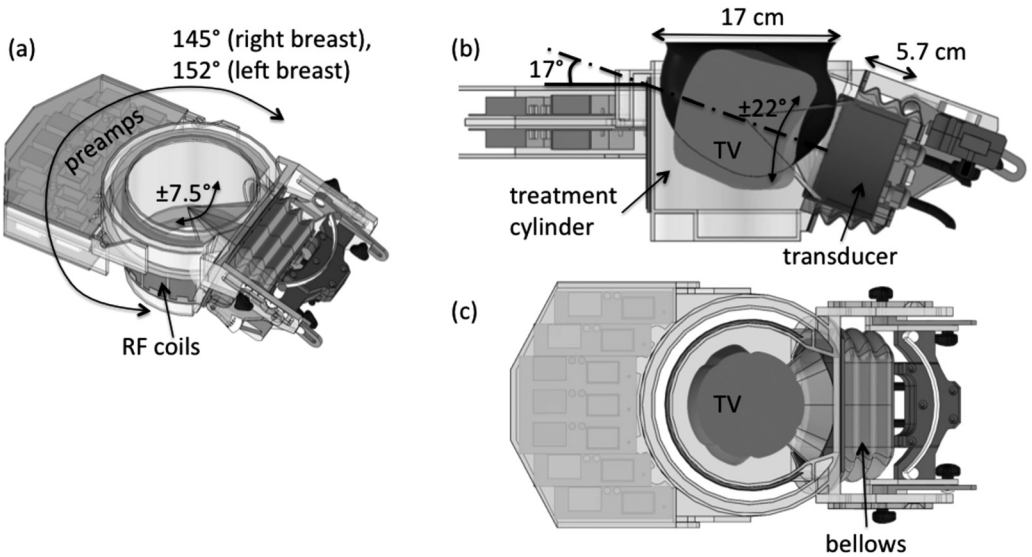

FIG. 3. (a) SolidWorks rendering of the transducer-cylinder assembly. The custom 11-channel RF coil array and associated pre-amplifiers are shown attached to the cylinder. The entire assembly can be rotated approximately 150° in a plane parallel to the scanner table. The transducer can be tilted an additional ±7.5° in the same plane and ±22° in the vertical plane around a nominal 17° tilt axis. (b) Side and (c) top views of the treatment volume (TV) within the cylinder that is possible using the limits imposed by the 60-cm diameter bore of the Siemens 3 T Trio MRI scanner. This volume includes the electronic steering capabilities of the transducer. A model of the breast shown in Fig. 10 is seen in Fig. 3(b).

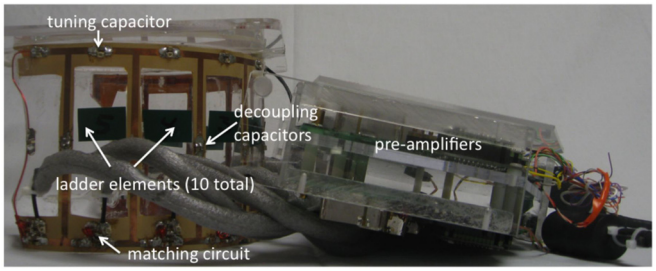

FIG. 4. Custom 11-channel RF-coil array removed from treatment cylinder assembly. Key coil components are identified.

as the ultrasound coupling fluid between the ultrasound transducer and breast. The volume of the cylinder is 3.25 L.

II.C. RF-coil array

Generally, the MRI RF-coil design for monitoring breast MRgHIFU treatments has been a single loop placed around the breast at the chest wall.[8,9,17] This single-loop design has some advantages since the single large coil provides a reasonably homogeneous signal profile, the coil placement does not interfere with the ultrasound beam propagation, and the coil is easily incorporated into the MRgHIFU device design. However, drawbacks to the single-loop coil design include its low SNR and the large inductance of the large coil size that causes frequency instability due to the decreased capacitance required to make the loop resonant. In addition, the deionized water that is used as the coupling fluid increases the capacitance of the system causing the frequency at which the coil resonates to be decreased, which requires the reduction of the capacitance necessary to resonate the coil at the frequency of 123 MHz. This resonance requirement for smaller capacitance therefore makes the loop more sensitive to variations in coil loading due to variations in patient size.

To improve image quality, our design incorporates an integrated 11-channel RF receiver coil that surrounds the treatment cylinder assembly,[25] as shown in Fig. 4. There are ten channels in a ladder-type configuration[26,27] that is wrapped from one edge of the treatment cylinder window around the cylinder to the other edge of the window. The ten elements are augmented by a 16.5-cm diameter single loop placed at the chest wall. This custom coil design was simulated and evaluated for a 3 T environment using Biot-Savart calculations implemented in MATLAB (Mathworks, Inc.). Simulations[28] were performed comparing the 11-channel coil performance with that of the single loop at the chest wall. Simulations were also performed to determine the effect of treatment cylinder radius on SNR at the center of the treatment cylinder. The SNR for eight different tank sizes was simulated using Biot-Savart calculations and corresponding coil and sample noise estimates. For each tank size, the number of coils spanning the circumference of the tank was held constant. Therefore, as the tank diameter increased, the size of the coils around the tank also increased. Experimentally, a comparison of the integrated 11-channel RF coil and 16.5-cm single-loop coil configurations was performed in a homogeneous phantom. Additionally, the repeatability of the temperature measurements for both configurations was evaluated in a nonheating test in a normal volunteer.

II.D. Experimental evaluation

All components of the system were designed to be MR compatible. There was no apparent image degradation due to the transducer or power generator system. SNR measurements were made while the power generator was off, when the power generator was on without supplying power to the transducer and when the transducer was active. In addition, the system was tested on both phantoms and ex vivo tissue samples before any human scans were performed. All components were found to be MRI compatible.

Testing was conducted on six normal volunteers to determine the length the breast was elongated during tensioning. In addition, the breast system design was evaluated for comfort inside a Siemens 3 T Trio MRI by 18 normal volunteers (15 female and 3 male). No medication was administered to the volunteers for these tests. Each volunteer spent approximately 60 min on the device, with a maximum of 120 min. The volunteers provided feedback regarding their comfort level every 15 min. All human testing was approved by the University of Utah's Internal Review Board.

The breast-specific MRgHIFU system was experimentally evaluated using both a homogenous phantom (ATS Laboratories, Bridgeport, CT, USA) and an inhomogeneous *ex vivo* porcine muscle tissue model. This model was composed of heterogeneous *ex vivo* porcine muscle that was placed in a breast-shaped mold. The mold was custom made by coating a positive breast-shaped plaster mold with several coats of

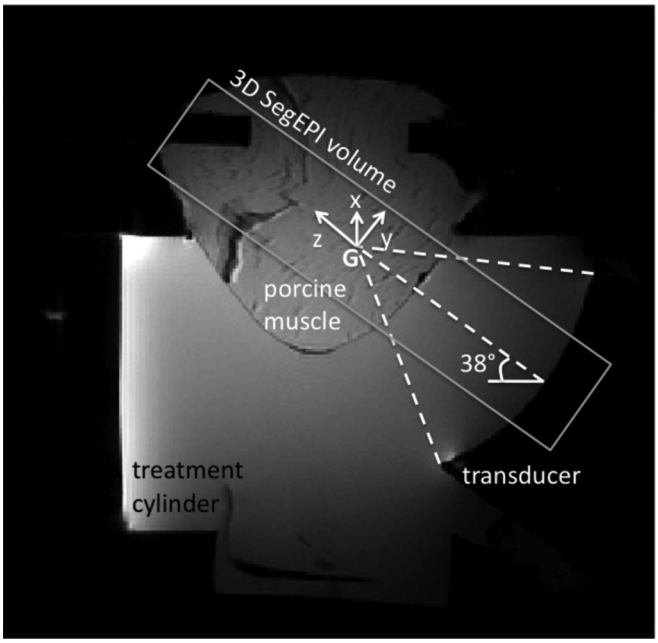

FIG. 5. Sagittal MRI image of experimental setup for the *ex vivo* porcine muscle model experiments. The transducer, water-filled cylinder and breast-shaped muscle sample are all seen. The 3D segmented EPI volume (parallel to the ultrasound beam propagation at an angle of 38° with respect to the horizontal) is indicated by the rectangle. The tilted x, y, z coordinate system used in all subsequent results has its origin at the geometric focus (G) of the transducer, as shown.

Plasti Dip (Blaine, MN, USA), a thin rubberized coating. For the homogeneous phantom experiments, sonications pulses of 42 acoustic watts (measured at the transducer face) for 30 s were applied at the geometric focus and also steered +1.5 cm in all directions.

For the heterogeneous *ex vivo* tissue model, experimental parameters were chosen to achieve an approximate temperature rise of 20 °C at the geometric focus. The experimental setup is shown in Fig. 5. In order to determine repeatability, five sonications were performed at the geometric focus in a single tissue model at 50 acoustic watts for 30 s. In additional heterogeneous *ex vivo* tissue models, single step inputs of ultrasound were applied at 70 acoustic watts (measured at the transducer face) for 30 s with the focal zone located at the transducer's geometric focus. Six additional sonications were executed with the beam steered away from the geometric focus ± 1.5 cm in each of the three coordinate axes. The tissue model was allowed to cool 10 min between all sonications. In addition to the individual sonication points, a volume was ablated using continuous sonication by executing the following path: Three planes were targeted, spaced 1 cm apart. In each plane, a 4×4 grid of sonication points with 2-mm spacing was treated for a total of 48 points. The spacing was selected based on the size of the focal spot (approximately 2×10 mm FWHM). The planes were treated back (furthest from the transducer face) to front and each point was sonicated for 10 s with 70 acoustic watts for a total sonication time of 8 min. The beam was electronically steered between all points. This experimental series was repeated in five different porcine muscle samples.

Finally, to gain an estimate of the repeatability of potential temperature measurements without heating present, one human volunteer was scanned with a 60-s duration of the temperature measurement sequence in the device with no ultrasonic power applied.

For all experiments, temperature measurements were acquired using the proton resonance frequency method[29,30] using the standard Siemens 3D segmented EPI sequence[31] with $128 \times 256 \times 64$ mm FOV, $64 \times 128 \times 32$ matrix, resulting in $2 \times 2 \times 2$ mm isotropic voxels. Other imaging parameters include TR/TE (ms): 23/12, FA: 25°, EPI factor = 9, echo spacing: 1.57 ms, bandwidth: 730 Hz/pixel, fat saturation used, frequency encode direction along the z-axis shown in Fig. 5, temporal resolution of 4.9 s per image volume. The reconstruction took into account noise variance by weighting each coil by the inverse of the noise variance. All images were postprocessed using zero-filled interpolation, resulting in 1-mm isotropic voxel spacing.[32] A temperature sensitivity coefficient of −0.01 ppm/ °C was used in all calculations. For all heating experiments, ultrasound sonication was initiated after the acquisition of a small number of baseline volumes and synchronized with the start of a volume acquisition.

III. RESULTS

As expected, the loss in SNR was very small when the generator was on and the transducer was firing and an even smaller loss in SNR was seen when the generator was on but the transducer was not firing. SNR measurements showed only a 1.9% drop in SNR when the power generator was on with the transducer not firing and a 2.5% drop when the transducer was firing.

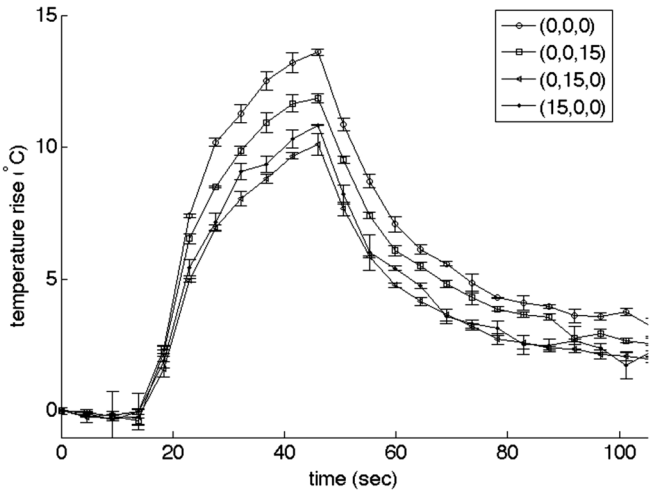

FIG. 6. Maximum temperature rise in a homogeneous phantom at four different locations (geometric focus and steered +15 mm in each coordinate direction) using 42 acoustic watts for 30 s. Three separate measurements were taken at each location. The error bars represent one standard deviation.

The results of the comfort testing by the 18 normal volunteers were generally positive. The experience of each individual varied, but all participants tolerated the device with negligible side effects. Minor complaints included slight shoulder and/or arm pain and neck stiffness. Most volunteers (13 females and 3 males) found lying face down (massage table-style) the most comfortable position; however, two females preferred to have their head to the side. For both of these positions, the height of the headrest was critical to the volunteer's comfort, so several settings were attempted before the final position was achieved. The tensioning tests showed that the breast could be elongated with no noticeable discomfort to the patient an average of 7 mm (std. dev. = 5 mm).

Figure 6 shows the mean maximum temperature rise and accompanying standard deviation (N = 3) in the homogeneous phantom with the beam focused at the geometric focus and steered off-axis +15 mm in all three directions individually. The error bars represent one standard deviation, ranging from 0.01 to 0.43 °C. The mean temperature response of several sonication pulses (N = 5) applied to the same location at the geometric focus in one of the heterogeneous *ex vivo* tissue samples is shown in Fig. 7(a). The standard deviation ranged from 0.14 to 0.62 °C. Less than 3% variability is seen in the temperature measurements at the same location for repeated sonications in the same tissue sample with the maximum temperature rise occurring at the same position in the sample. The starting temperature of the heterogeneous *ex vivo* tissue sample for each of these measurements was 22 °C; therefore, the absolute maximum temperature rise was approximately 47 °C and no significant thermal dose was accumulated in the heterogeneous *ex vivo* tissue model during repeated experiments.

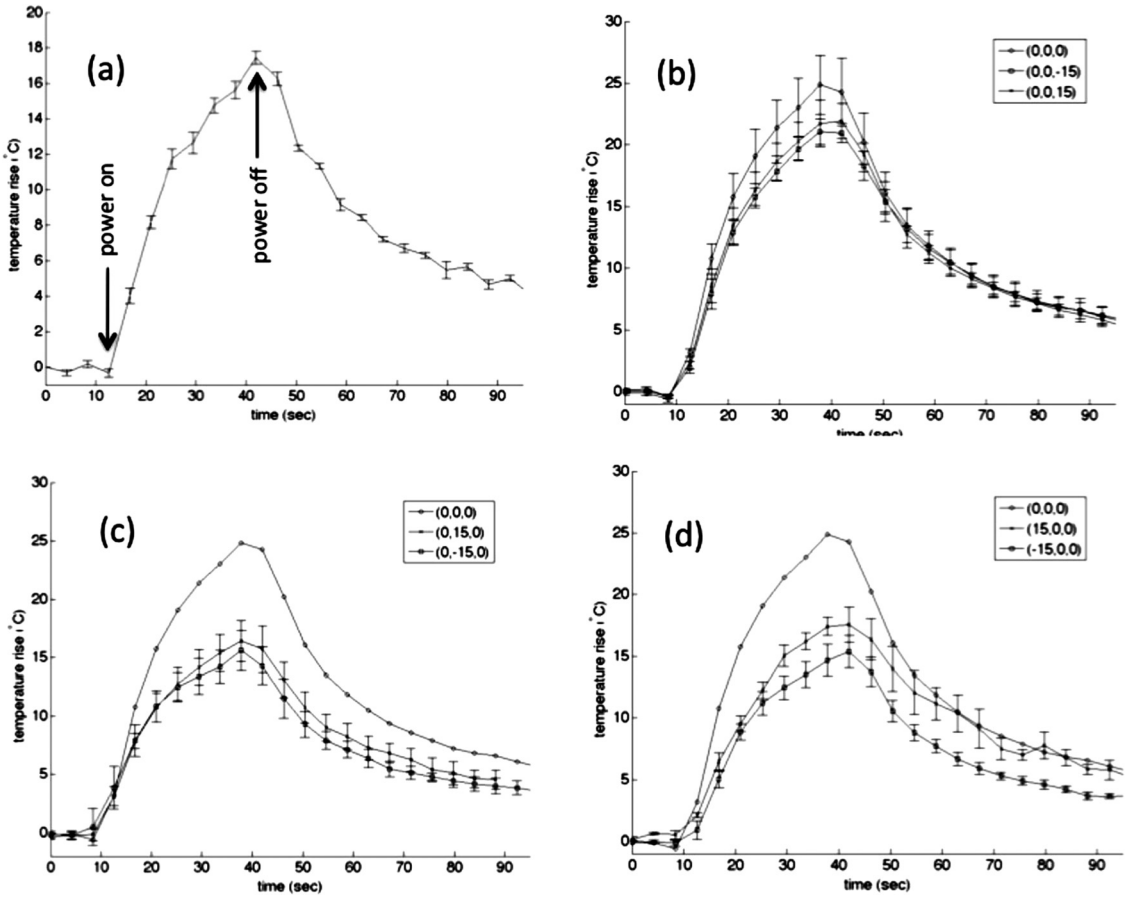

FIG. 7. (a) Maximum temperature rise at the geometric focus in one *ex vivo* porcine tissue sample when the ultrasound beam was unsteered using 50 acoustic watts for 30 s. Five separate measurements were taken. The error bars represent one standard deviation. (b)–(d) Mean temperature rise at the hottest voxel in five different porcine muscle samples when the beam was focused at the geometric focus and steered ±15 mm in each coordinate direction using 70 acoustic watts. The steered distance is represented as (Δy,Δx,Δz). The error bars in all plots represent the standard deviation. Mean temperature with beam steered at (b) geometric focus, (0,0,15) and (0,0,−15); (c) geometric focus (with error bars removed), (0,15,0), (0,−15,0); (d) geometric focus, (15,0,0), (−15,0,0).

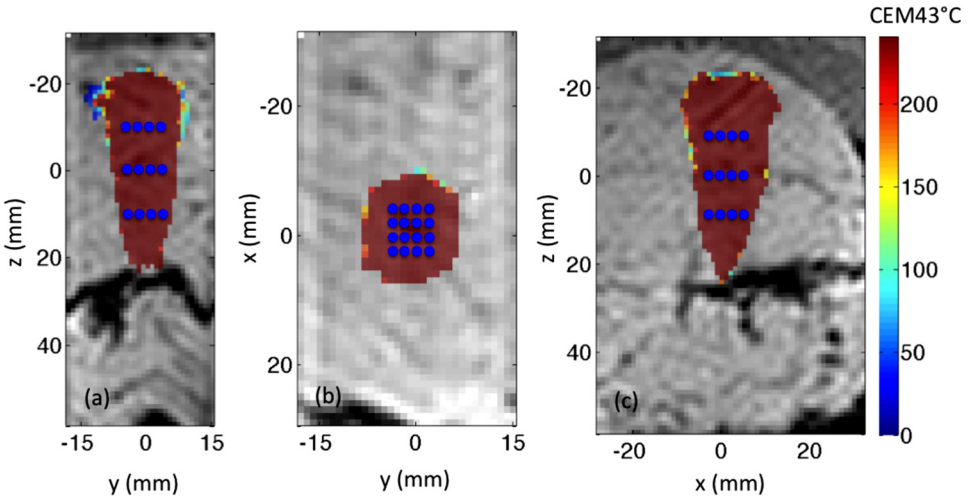

FIG. 8. Views of the volume of tissue that received at least 240 CEM43 °C after the execution of the predefined path, as shown in the (a) y-z at x = 0, (b) x-y at z = 0, and (c) x-z at y = 0 planes for one of the porcine tissue samples. The coordinate system orientation is defined in Fig. 5. The thermal dose accumulated is overlaid on the magnitude image. The scale is the same for all images. The total volume that received at least 240 CEM43 °C after 8 min of heating in this particular tissue was 7.9 cm^3. The transducer is located at the top of images (a) and (c) and into the page for image (b). The blue dots represent the locations of each sonication path point.

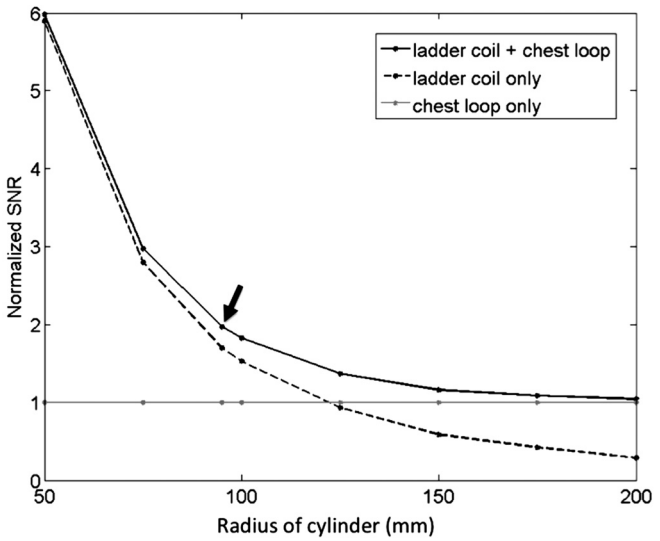

FIG. 9. Normalized SNR for the 11-channel RF-coil array (ten-channel ladder coil plus the single-loop chest coil), simulated at the center of the treatment cylinder as a function of cylinder radius. The radius of the RF-coil mounted around the treatment cylinder shown in Fig. 1 is 95 mm, as indicated by the arrow.

Figures 7(b)–7(d) displays the mean temperature response for each of five porcine muscle samples when the beam was focused at the geometric focus and steered away from the geometric focus by ± 1.5 cm in each of the three Cartesian directions (coordinate system shown in Fig. 5). The data corresponding to steering in the z-direction are shown in Fig. 7(b) and in the x-direction and y-direction are shown in Figs. 7(c) and 7(d), respectively. The ratio of maximum temperature achieved at each of the steered positions to the maximum temperature reached at the geometric focus ranged from 0.61 when steered in the negative x-direction to 0.88 when steered in the positive z-direction.

An example of the ablated volume in one porcine muscle sample after executing the predefined path, as described in Sec. II, is shown in Fig. 8. The origin in the figures denotes the geometric focus of the transducer. When assuming the starting temperature of the tissue sample was 37 °C, the total volume that received a minimum thermal dose of 240 CEM43 °C was 7.9 cm^3 in this particular example. The mean of the total volume that received at least 240 CEM43 °C during the ablation period for all five tissue samples was 8.17 cm^3 (standard deviation of 0.35 cm^3).

Figure 9 shows the SNR (normalized to the single-loop coil configuration) for the 11-channel RF-coil system as simulated at the center of the treatment cylinder as a function of cylinder radius. The normalized SNR for the single-loop chest coil and ten-channel ladder coil array are also shown. The radius of the device described in this paper is 85 mm, resulting in a RF-coil radius of 95 mm, one of the simulated sizes. Experimentally, in a homogeneous phantom, it was found that the mean relative SNR for the 11-channel RF-coil array was 61% greater than the relative SNR seen with just the single-loop coil. An example of the performance of the 11-channel array compared to a single loop at the chest wall is shown in Fig. 10 for a normal volunteer. The precision of the temperature measurements achieved using the 11-channel array compared to a single-loop coil can be gauged by the standard deviation of temperature measurements taken during a 60-s period with no ultrasound heating. When using the 11-channel RF-coil array, there was a 62% increase in temperature accuracy in the voxels containing aqueous tissue when compared to the accuracy achieved with the single-loop coil alone.

IV. DISCUSSION

The breast-specific MRgHIFU device presented here has several features designed to enable clinicians to perform safe and effective treatments in a wide variety of breast cancer cases. To maximize the likelihood of successful treatments, the device was designed for comfort, flexibility in treatment steering, and improved temperature accuracy and repeatability for improved treatment control. The device was specifically designed to reduce the water volume required to couple the ultrasound from the transducer to the breast and still allow the ultrasound beam focus to be positioned such that the majority of breast lesions could be treated. It should be noted that this device is not able to treat any lesions in the axilla since the available treatment volume only includes tissue suspended in the treatment cylinder.

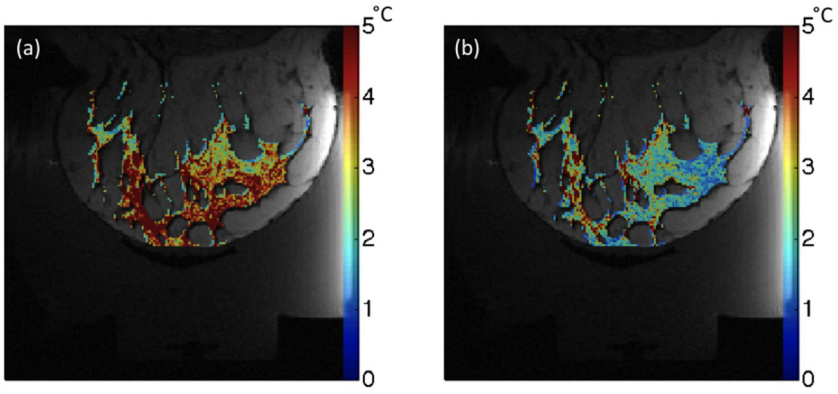

FIG. 10. Standard deviation of temperature measurements in the breast of a normal volunteer during a 60-s nonheating test. The temperature variation is shown in the water-based tissues only. (a) Variation seen using a single-loop RF coil around the chest wall. (b) Variation seen using the entire 11-channel RF-coil array.

Patient comfort is always a difficult problem for prolonged time periods, particularly inside an MRI where movement is limited and discouraged during treatments. Previous treatment times in the literature for breast MRgHIFU range from 45 min for small lesions (1 cm) to 150 min for larger lesions (>3 cm).[8,13] The actual time spent in the magnet will be longer when positioning, registration and preimaging and postimaging time is added to the ablation times reported above. Therefore, significant efforts were spent in maximizing the comfort of the breast MRgHIFU device as this could be a limiting factor in future clinical tests.

The treatment cylinder (Fig. 3) isolates the breast that will be treated by removing all critical tissues including the nipple, ribs and lungs from the ultrasound propagation path, and allows the ultrasound focal point to treat 50% of the entire treatment cylinder volume. The transducer is located outside the cylinder and is able to move 5.7 cm away and toward the breast [as seen in Fig. 3(b)] to adjust to differing breast sizes and tumor locations. The treatment cylinder also allows the transducer to be rotated in two planes (Fig. 3). This additional flexibility will enable the treatment of tumors closer to the chest wall. Additionally, the angle of ultrasound beam propagation [the 17° angle shown in Fig. 3(b)] is made as small as possible by elongation of the treated breast through use of the tensioning device seen in Fig. 2. While tilting the transducer at the most extreme angles toward vertical will place the chest wall partially in the far-field region of the ultrasound beam, this is still a significant improvement when compared to devices that propagate the ultrasound beam vertically from below the breast. During ablation, while some heating and subsequent ablation does occur in the near field of the ultrasound beam due to absorption and the electronic steering of the beam,[33] there is minimal thermal dose that accumulates in the far field of the beam, as seen in Fig. 8.

The use of the 17-cm cylinder reduces the water volume and thereby reduces image noise. Further, the cylinder radius is sufficiently small that RF receiver coils placed on the cylinder can be used to increase the image SNR over that of the chest loop alone. Because the transducer is positioned in a window that passes into the cylinder, the RF-coil array can only occupy about 75% of the cylinder circumference. However, that is sufficient for placement of a ten-channel RF-coil array directly on the surface of the treatment cylinder without blocking the ultrasound acoustic window. Figure 10 shows the significant increase in temperature accuracy that is achievable with this coil when combined with a single-loop chest coil. While tissue near the chest wall, and hence, near the single-loop chest coil, may have adequate SNR for temperature measurements, larger breasts will be more difficult to monitor accurately without the addition of the other ten channels. This feature will improve both the efficacy and safety of MRgHIFU breast treatments. In addition, phased-array RF coils allow for the possibility for parallel imaging to monitor MRgHIFU treatments.[25] Other groups[34] have investigated using immersed, thin RF coils to increase sensitivity during MRgHIFU treatments. The incorporation of immersed coils in front of the transducer may further increase SNR in the breast, particularly in the near field of the ultrasound beam.

The results shown in Figs. 7 and 8(a) demonstrate the repeatability of the breast system. The standard deviation of the temperature measurement was small for both the homogeneous phantom ($\sigma = 0.01-0.43\,^{\circ}\mathrm{C}$) and inhomogeneous *ex vivo* tissue model ($\sigma = 0.14-0.62\,^{\circ}\mathrm{C}$) between repeated ultrasound sonications in the same location in a single sample. The intertissue sample measurements, as seen in Figs. 7(b)–7(d) did have more variability in the temperature measurements as well as in the volume of tissue ablated using the predefined path described in Sec. II. This increased variability over that observed in repeated heating of a single sample [Fig. 7(a)] is probably due to differences in the tissue samples, corresponding to patient-to-patient variations that will be present in clinical treatments. The percentage of fat present in each tissue preparation varied from sample to sample, and published tissue property values vary significantly for muscular tissue, with attenuation coefficients ranging from 0.055 to 0.12 Np/cm at 1 MHz.[35] Simulations of heating the segmented tissue model for 30 s at 70 acoustic watts show that the resulting temperature rise from the same sample using two different attenuation values for muscle (0.05 and 0.12 Np/cm) at the geometric focus of the transducer results in a 6.3 °C difference. Therefore, the larger variability in these measurements is most likely due to intertissue variability instead of system variation.

Along with the many advantages of this breast MRgHIFU system, there are a few notable limitations. This system was designed to sit on top of the existing MRI patient table. The total height of the system is 17 cm, and this limits the size of patient that can be treated in a 60-cm bore MRI system. Even with relatively slender patients, the fit is quite snug in the MRI bore and can exacerbate any claustrophobic reaction patients may experience. This was not the case with the 18 volunteers that participated in the device testing, but would most likely be somewhat problematic in a larger population. This size limitation will be greatly reduced when the device is used in the newer generation of 70-cm bore MRI scanners. Further, in the current device design, the transducer must be manipulated manually. This design did not incorporate any motors to allow remote control of the transducer position. Thus, without manual repositioning, this limits the treatment volume to about 3 cm in diameter with electronic steering. If multiple tumors are to be targeted, the transducer must be moved manually. The design of the patient support platform does allow the operator to reposition the transducer for a new treatment location without removing the patient from the device, but the requirement of new localizer scans and the need to make repeated adjustments may potentially lengthen the total treatment time beyond a reasonable limit. The future addition of a motor driven transducer positioning system should partially alleviate this problem.

V. CONCLUSIONS

The overall design and characterization of a new breast-specific MRgHIFU system have been presented. This design incorporates many features that will enable safer and more efficacious treatments of breast tumors with focused

ultrasound. Key design improvements include a laterally shooting phased-array transducer, a treatment cylinder that isolates the treated breast in reduced water volume, and an integrated 11-channel RF receiver coil that provides increased SNR resulting in faster, more accurate temperature measurements. This design will potentially allow the treatment of a wider population of breast tumors.

ACKNOWLEDGMENTS

The authors gratefully acknowledge support from Siemens Healthcare AG, Image Guided Therapy, the Ben and Iris Margolis Foundation and NIH-1-R01-CA134599.

[a]Author to whom correspondence should be addressed. Electronic mail: apayne@ucair.med.utah.edu

[1]T. Bohm, I. Hilger, W. Muller, J. R. Reichenbach, M. Fleck, and W. A. Kaiser, "Saline-enhanced radiofrequency ablation of breast tissue: An in vitro feasibility study," Invest. Radiol. **35**(3), 149–157 (2000).

[2]S. S. Jeffrey, R. L. Birdwell, D. M. Ikeda, B. L. Daniel, K. W. Nowels, F. M. Dirbas, and S. M. Griffey, "Radiofrequency ablation of breast cancer: first report of an emerging technology," Arch. Surg. **134**(10), 1064–1068 (1999).

[3]M. A. Hall-Craggs, "Interventional MRI of the breast: Minimally invasive therapy," Eur. Radiol. **10**(1), 59–62 (2000).

[4]S. A. Harries, Z. Amin, M. E. Smith, W. R. Lees, J. Cooke, M. G. Cook, J. H. Scurr, M. W. Kissin, and S. G. Bown, "Interstitial laser photocoagulation as a treatment for breast cancer," Br. J. Surg. **81**(11), 1617–1619 (1994).

[5]R. W. Rand, R. P. Rand, F. Eggerding, L. DenBesten, and W. King, "Cryolumpectomy for carcinoma of the breast," Surg. Gynecol. Obstet. **165**(5), 392–396 (1987).

[6]E. D. Staren, M. S. Sabel, L. M. Gianakakis, G. A. Wiener, V. M. Hart, M. Gorski, K. Dowlatshahi, B. F. Corning, M. F. Haklin, and G. Koukoulis, "Cryosurgery of breast cancer," Arch Surg. **132**(1), 28–33 (1997); discussion 34.

[7]M. Oka, T. Okumura, H. Yokoi, T. Murao, Y. Miyashita, K. Ota, S. Yoshitatsu, K. Yoshioka, H. Hirano, and Y. Kawashima, "Surgical application of high intensity focused ultrasound," Med. J. Osaka Univ. **10**(3–4), 427–442 (1960).

[8]K. Hynynen, O. Pomeroy, D. N. Smith, P. E. Huber, N. J. McDannold, J. Kettenbach, J. Baum, S. Singer, and F. A. Jolesz, "MR imaging-guided focused ultrasound surgery of fibroadenomas in the breast: A feasibility study," Radiology **219**(1), 176–185 (2001).

[9]P. E. Huber, J. W. Jenne, R. Rastert, I. Simiantonakis, H. P. Sinn, H. J. Strittmatter, D. von Fournier, M. F. Wannenmacher, and J. Debus, "A new noninvasive approach in breast cancer therapy using magnetic resonance imaging-guided focused ultrasound surgery," Cancer Res. **61**(23), 8441–8447 (2001).

[10]D. Gianfelice, A. Khiat, M. Amara, A. Belblidia, and Y. Boulanger, "MR imaging-guided focused US ablation of breast cancer: Histopathologic assessment of effectiveness—Initial experience," Radiology **227**(3), 849–855 (2003).

[11]F. Wu, Z. B. Wang, Y. D. Cao, Z. L. Xu, Q. Zhou, H. Zhu, and W. Z. Chen, "Heat fixation of cancer cells ablated with high-intensity-focused ultrasound in patients with breast cancer," Am. J. Surg. **192**(2), 179–184 (2006).

[12]H. Furusawa, K. Namba, H. Nakahara, C. Tanaka, Y. Yasuda, E. Hirabara, M. Imahariyama, and K. Komaki, "The evolving non-surgical ablation of breast cancer: MR guided focused ultrasound (MRgFUS)," Breast Cancer **14**(1), 55–58 (2007).

[13]H. Furusawa, K. Namba, S. Thomsen, F. Akiyama, A. Bendet, C. Tanaka, Y. Yasuda, and H. Nakahara, "Magnetic resonance-guided focused ultrasound surgery of breast cancer: Reliability and effectiveness," J. Am. Coll. Surg. **203**(1), 54–63 (2006).

[14]F. Wu, Z. B. Wang, Y. D. Cao, X. Q. Zhu, H. Zhu, W. Z. Chen, and J. Z. Zou, ""Wide local ablation" of localized breast cancer using high intensity focused ultrasound," J. Surg. Oncol. **96**(2), 130–136 (2007).

[15]F. Wu, Z. B. Wang, W. Z. Chen, W. Wang, Y. Gui, M. Zhang, G. Zheng, Y. Zhou, G. Xu, M. Li, C. Zhang, H. Ye, and R. Feng, "Extracorporeal high intensity focused ultrasound ablation in the treatment of 1038 patients with solid carcinomas in China: An overview," Ultrason. Sonochem. **11**(3–4), 149–154 (2004).

[16]F. Wu, Z. B. Wang, H. Zhu, W. Z. Chen, J. Z. Zou, J. Bai, K. Q. Li, C. B. Jin, F. L. Xie, and H. B. Su, "Extracorporeal high intensity focused ultrasound treatment for patients with breast cancer," Breast Cancer Res. Treat. **92**(1), 51–60 (2005).

[17]D. Gianfelice, A. Khiat, Y. Boulanger, M. Amara, and A. Belblidia, "Feasibility of magnetic resonance imaging-guided focused ultrasound surgery as an adjunct to tamoxifen therapy in high-risk surgical patients with breast carcinoma," J. Vasc. Interv. Radiol. **14**(10), 1275–1282 (2003).

[18]C. S. Ho, K. C. Ju, T. Y. Cheng, Y. Y. Chen, and W. L. Lin, "Thermal therapy for breast tumors by using a cylindrical ultrasound phased array with multifocus pattern scanning: A preliminary numerical study," Phys. Med. Biol. **52**(15), 4585–4599 (2007).

[19]K. C. Ju, L. T. Tseng, Y. Y. Chen, and W. L. Lin, "Investigation of a scanned cylindrical ultrasound system for breast hyperthermia," Phys. Med. Biol. **51**(3), 539–555 (2006).

[20]C. Mougenot, M. O. Kohler, M. Tillander, C. Moonen, W. Bartels, and G. J. Ehnholm, "Large aperture transducer designed for MR-HIFU treatment of breast tumors," *International Society of Magnetic Resonance in Medicine* (2011), Montreal, Canada, p. 1727.

[21]E. S. Ebbini and C. A. Cain, "Multiple-focus ultrasound phased-array pattern synthesis: Optimal driving-signal distributions for hyperthermia," IEEE Trans. Ultrason. Ferroelectr. Freq. Control **36**(5), 540–548 (1989).

[22]C. L. Carter, C. Allen, and D. E. Henson, "Relation of tumor size, lymph node status, and survival in 24,740 breast cancer cases," Cancer **63**(1), 181–187 (1989).

[23]L. R. Gavrilov and J. W. Hand, "A theoretical assessment of the relative performance of spherical phased arrays for ultrasound surgery," IEEE Trans. Ultrason. Ferroelectr. Freq. Control **47**(1), 125–139 (2000).

[24]S. A. Goss, L. A. Frizzell, J. T. Kouzmanoff, J. M. Barich, and J. M. Yang, "Sparse random ultraosund phased array for focal surgery," IEEE Trans Ultrason. Ferroelectr. Freq. Control **43**(6), 1111–1121 (1996).

[25]E. Minalga, A. Payne, R. Merrill, N. Todd, S. Vijayakumar, E. Kholmovski, D. Parker, and J. Hadley, "An 11-channel phased array radio frequency coil array for magnetic resonance guided high intensity focused ultrasound of the breast," Magn. Reson. Med. (accepted).

[26]J. Jetvic, IGC—Medical Advances, Inc., assignee, "Phased array local coil for MRI imaging having non-overlapping regions of sensitivity," U.S. patent 7,091,721 (2006).

[27]J. Wang, "A novel metod to reduce the signal coupling of surface coils for MRI," *International Society of Magnetic Resonance in Medicine* (1996), New York, p. 1434.

[28]E. Minalga, A. Payne, R. Merrill, N. Todd, S. Vijayakumar, D. Parker, and J. Hadley, "Design and evaluation of RF coils for magnetic resonance guided high intensity focused ultrasound," *International Society of Magnetic Resonance in Medicine* (2011), Montreal, Canada, p. 1726.

[29]Y. Ishihara, A. Calderon, H. Watanabe, K. Okamoto, Y. Suzuki, K. Kuroda, and Y. Suzuki, "A precise and fast temperature mapping using water proton chemical shift," Magn. Reson. Med. **34**(6), 814–823 (1995).

[30]J. De Poorter, C. De Wagter, Y. De Deene, and C. Thomsen, "The proton resonance frequency shift method compared with molecular diffusion for quantitative measurement of two-dimensional time-dependent temperature distribution in a phantom," J. Magn. Reson., Ser. B **103**, 234–241 (1994).

[31]A. Kickhefel, J. Roland, C. Weiss, and F. Schick, "Accuracy of real-time MR temperature mapping in the brain: A comparison of fast sequences," Phys. Med. **26**(4), 192–201 (2010).

[32]N. Todd, U. Vyas, J. de Bever, A. Payne, and D. L. Parker, "The effects of spatial sampling choices on MR temperature measurements," Magn. Reson. Med. **65**(2), 515–521 (2011).

[33]A. Payne, U. Vyas, N. Todd, J. de Bever, D. A. Christensen, and D. L. Parker, "The effect of electronically steering a phased array ultrasound transducer on near-field tissue heating," Med. Phys. **38**(9), 4971–4981.

[34]M. Rata, R. Salomir, R. Umathum, J. Jenne, C. Lafon, F. Cotton, and M. Bock, "Endoluminal ultrasound applicator with an integrated RF coil for high-resolution magnetic resonance imaging-guided high-intensity contact ultrasound thermotherapy," Phys. Med. Biol. **53**(22), 6549–6567 (2008).

[35]C. F. Andrew, "Tissue Substitutes, Phantoms and Computational Modelling in Medical Ultrasound," Report No. 61 (International Commission on Radiation Units and Measurements, 1998).